FP7-600716

Whole-Body Compliant Dynamical Contacts in Cognitive Humanoids

D5.4
Validation scenario 4: learning how to stand up with the help of a human caregiver.

Editor(s)	Francesco Nori
Responsible Partner	IIT
Affiliations	[1] IIT
Status-Version:	Draft-1.0
Date:	Feb. 28, 2017
EC Distribution:	Consortium
Project Number:	600716
Project Title:	Whole-Body Compliant Dynamical Contacts in Cognitive Humanoids

Title of Deliverable:	Validation scenario 4: learning how to stand up with the help of a human caregiver.
Date of delivery to the EC:	28/2/2017

Workpackage responsible for the Deliverable	deliv WP5
Editor(s):	Francesco Nori
Contributor(s):	Daniele Pucci, Francesco Romano, Jorhabib Eljaik, Silvio Traversaro, Vincent Padois, Francesco Nori, Claudia Latella, Marta Lorenzini, Maria Lazzaroni, Oriane Dermy, Serena Ivaldi, Alexandros Paraschos, Olivier Rochel
Reviewer(s):	
Approved by:	All Partners

Abstract	This deliverable discusses the technical details and choices for the implementation of the year-4 validation scenario of the CoDyCo project. The validation scenario aims at validating the theoretical results in robot whole-body control while interacting with humans. Physical human-robot interaction is a field of growing interest among the scientific community. One of the main challenges is to replicate the physical mutual interaction occurring during human-human collaborative tasks. For this purpose, the knowledge about human whole-body motions and forces is mandatory but the current state of the art on robots ability in estimating them is not sufficient to yield to a suitable interaction. This deliverable presents a human-robot physical interaction task and exploits a wearable technology to monitor humans dynamics during the interaction
Keyword List:	Whole-body human dynamics, Human-robot physical collaboration, Probabilistic sensor fusion algorithm

Document Revision History

Version	Date	Description	Author
First draft	19 Feb 2017	In this version we simply write down a few considerations on the fourth year validation scenario as discussed after the mid-year CoDyCo meeting in Nancy.	Francesco Nori
Final version	27 Feb 2017	None	Francesco Nori

Table of Contents

1 Introduction

The understanding of the human dynamics and the way in which its contribute can be applied to enhance a physical human-robot interaction (pHRI) are two of the most promising challenges for the scientific community due mainly to their enormous and to-be-developed potential in industrial scenarios, ergonomics context, as well as in assistive and rehabilitation fields. Classical robots are built to act *for* humans, but in order to adapt their functionality to the current technological progress, the new generation of robots will have to collaborate *with* humans. This implies that the robots will be endowed with the capability to control physical collaboration through intentional interaction with humans. To achieve this condition, robots have to know mandatorily the dynamics (contact forces, internal forces, joint torques) of the human agent who they are interacting with. However the current state of the robot knowledge in observing human whole-body dynamics yields to non-proficient and unadaptive interactions.

To overcome this drawback, it is fundamental to understand what the response of the human body is while a physical interaction is occurring. The importance in retrieving this information is exemplified in Fig. 1: once the dynamic variables are computed by exploiting a dynamics estimation algorithm, the human dynamics feedback may be provided to the robot controllers. As a consequence, the robot may adjust the strategy of interaction accordingly.

This work is the first attempt to go in this direction since a first pHRI task was inserted with respect to our previous work [10] where only an investigation on the human inverse dynamics was carried out. The paper is built on the theoretical framework described in [10] from which it inherits both the notation and formulation.

The paper is structured as follows. Section 2 introduces the state-of-the-art background which the paper is based on. Section 3 presents the modelling of the human body as an articulated multi-body system. In Section 4 the adopted Gaussian probabilistic domain for the sensor fusion methodology is briefly recalled. Section 5 outlines the experimental set-up followed by a description of the results in Section 6. Conclusions and several considerations on the pivotal role of further control and estimation developments are depicted in Section 7.

2 Background

The aim of this Section is to provide a rapid fast-forward of what is the current direction of the scientific community on this topic. Most of the studies on the pHRI take inspiration from the intrinsic behaviour of the human nature: the *mutual adaptive nature* that automatically occurs when two humans are cooperating together to accomplish a common task.

To this purpose, the importance of understanding human dynamics goes without saying and it is a crucial aspect of current state-of-the-art studies. Since humans move by minimizing jerk trajectories [5], a method based on the minimum jerk model is used as a suitable approximation for estimating the human partner motions in [11]. Here the attempt is that of incorporating human characteristics in the control strategy of the

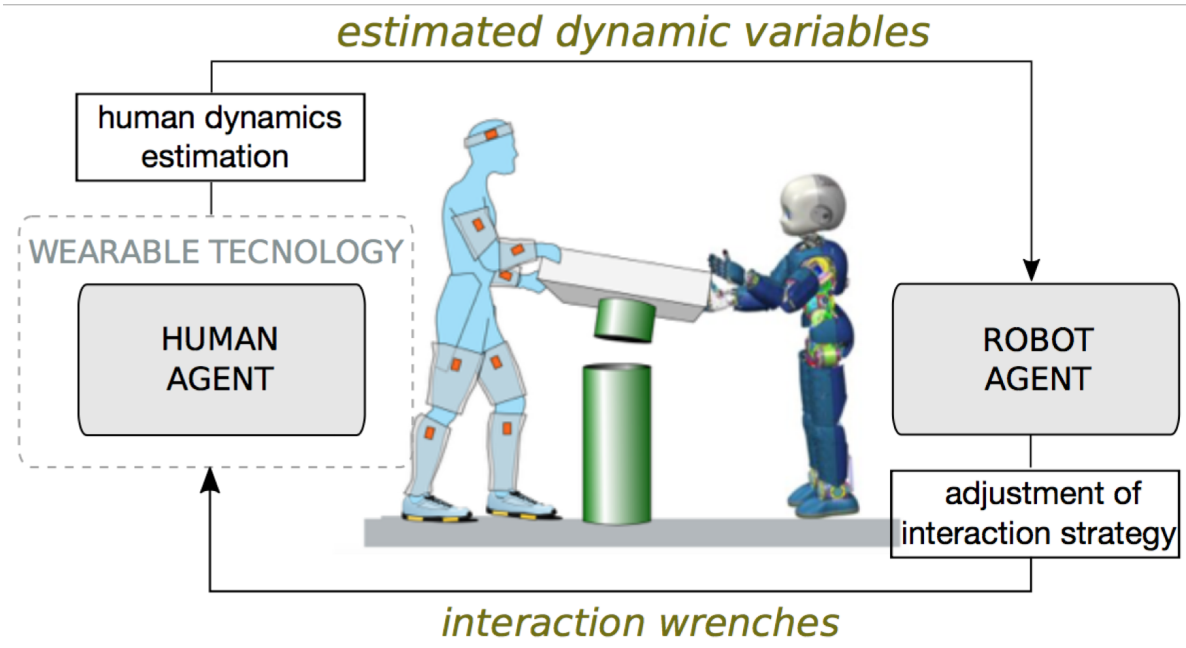

Figure 1: An example of pHRI scenario: the human agent is provided with a wearable technology and an estimation algorithm allows to retrieve information about his dynamics. By properly embedding estimations in the control loop of the robot, the intentional collaboration may be enhanced.

robot. The weakness in this type of approach, however, lies in the pre-determination of the task and in the role that the robot has to play in the task execution. Furthermore, the minimum jerk model reliability decreases considerably if the human partner decides to apply non-scheduled trajectory changes during the task [15]. Another route for pHRI is the *imitation learning* approach, where the movements of two human actors are typically retrieved with motion capture techniques, clustered in motion database ([6], [9], [22]) and then used to learn the interaction skills ([1], [20], [12]).

2.1 Problem statement

Unlike the current leaning, we want to pay more attention on the key role that a proper sensing technology for human beings together with dynamics estimation algorithms may offer for retrieving whole-body motions and interaction forces. More in detail, our work will be based on the formalism adopted for humanoid robots by making the assumption of modelling the human body as a articulated rigid multi-body system. The advantage of this choice is evident since it allows to handle both systems with the same mathematical tools. In this domain, the application of the Euler-Poincaré formalism [13] leads to three sets of equations describing: $i)$ the motion of the robot, $ii)$ the motion characterizing the human, $iii)$ the linking equations characterizing the contacts between human and robot.

$$i) \quad \mathbf{M}(\boldsymbol{q})\dot{\boldsymbol{v}} + \mathbf{C}(\boldsymbol{q},\boldsymbol{v})\boldsymbol{v} + \mathbf{G}(\boldsymbol{q}) = \begin{bmatrix} \mathbf{0} \\ \boldsymbol{\tau} \end{bmatrix} + \mathbf{J}^{\top}(\boldsymbol{q})\mathbf{f}$$

$$ii) \quad \mathbb{M}(\bar{\boldsymbol{q}})\dot{\bar{\boldsymbol{v}}} + \mathbb{C}(\bar{\boldsymbol{q}}, \bar{\boldsymbol{v}})\bar{\boldsymbol{v}} + \mathbb{G}(\bar{\boldsymbol{q}}) = \begin{bmatrix} \mathbf{0} \\ \boldsymbol{\tau} \end{bmatrix} + \mathbb{J}^{\top}(\bar{\boldsymbol{q}})\mathbf{f}$$

$$iii) \quad \begin{bmatrix} \mathbf{J}(\boldsymbol{q}) & \mathbb{J}(\bar{\boldsymbol{q}}) \end{bmatrix} \begin{bmatrix} \dot{\boldsymbol{v}} \\ \dot{\bar{\boldsymbol{v}}} \end{bmatrix} + \begin{bmatrix} \dot{\mathbf{J}}(\boldsymbol{q}) & \dot{\mathbb{J}}(\bar{\boldsymbol{q}}) \end{bmatrix} \begin{bmatrix} \boldsymbol{v} \\ \bar{\boldsymbol{v}} \end{bmatrix} = \mathbf{0}$$

Equations $i)$ and $ii)$ are floating base system representations of the dynamics of the robot and human models, respectively. Vectors $\boldsymbol{q}$ and $\bar{\boldsymbol{q}}$ represent the configuration space (i.e. the position and orientation of a chosen frame, called base frame, and the joints configuration) of the two systems. The velocity is represented by $\boldsymbol{v}$ and $\bar{\boldsymbol{v}}$ for robot and human systems, respectively. The matrices M, C, G and $\mathbb{M}$, $\mathbb{C}$, $\mathbb{G}$ denote the mass matrix, Coriolis matrix and the gravity bias term for the robot and the human systems, respectively. The forces the two systems exchange are denoted by $\mathbf{f}$, which owns a proper dimension depending on the number of wrenches[1] exchanged during the interaction task[2]. The Jacobians associated with the forces $\mathbf{f}$ are denoted by $\mathbf{J}(\mathbf{q})$ and $\mathbb{J}(\bar{\boldsymbol{q}})$. In $iii)$ we make the assumption of rigid contacts between the two systems.

3 Human Body Modelling

We propose a human body reference model as an articulated multi-body skeleton with rigid bodies connected by 3 Degrees-of-Freedom (DoF) joints. Kinematic and dynamic properties are defined as follows.

3.1 Kinematic properties

Inspired by the biomechanical model developed for the Xsens MVN motion capture system [19] shown in Fig. 3b, our model consists of a set of 23 rigid bodies with simple geometric shapes (parallelepiped, cylinder, sphere). The origin of each link is located at the parent joint origin, (i.e., the joint that connects the link to its parent). Figure 2b shows links and joints of the model. The dimension of each link is estimated by using data coming from motion capture acquisition.

3.2 Dynamic properties

The dynamic properties, such as center of mass and inertia tensor for each link, are not embedded in the Xsens output data since they are usually computed in a post-processing phase. Since our aim is to have a real-time estimation for the human dynamic variables, the knowledge of dynamic properties during the acquisition phase is

[1] As an abuse of notation, we define as wrench a quantity that is not the dual of a twist but a vector $\in \mathbb{R}^6$ containing both the forces and the related moments.

[2] For the sake of simplicity, we omitted the forces the two systems exchange with the external environment (i.e., the ground) from the formulation of $i)$ and $ii)$. As a straightforward consequence, the linking equations between each system with the external environment are not considered.

[3] The RGB (Red-Green-Blue) convention for x-y-z axes is adopted throughout the paper.

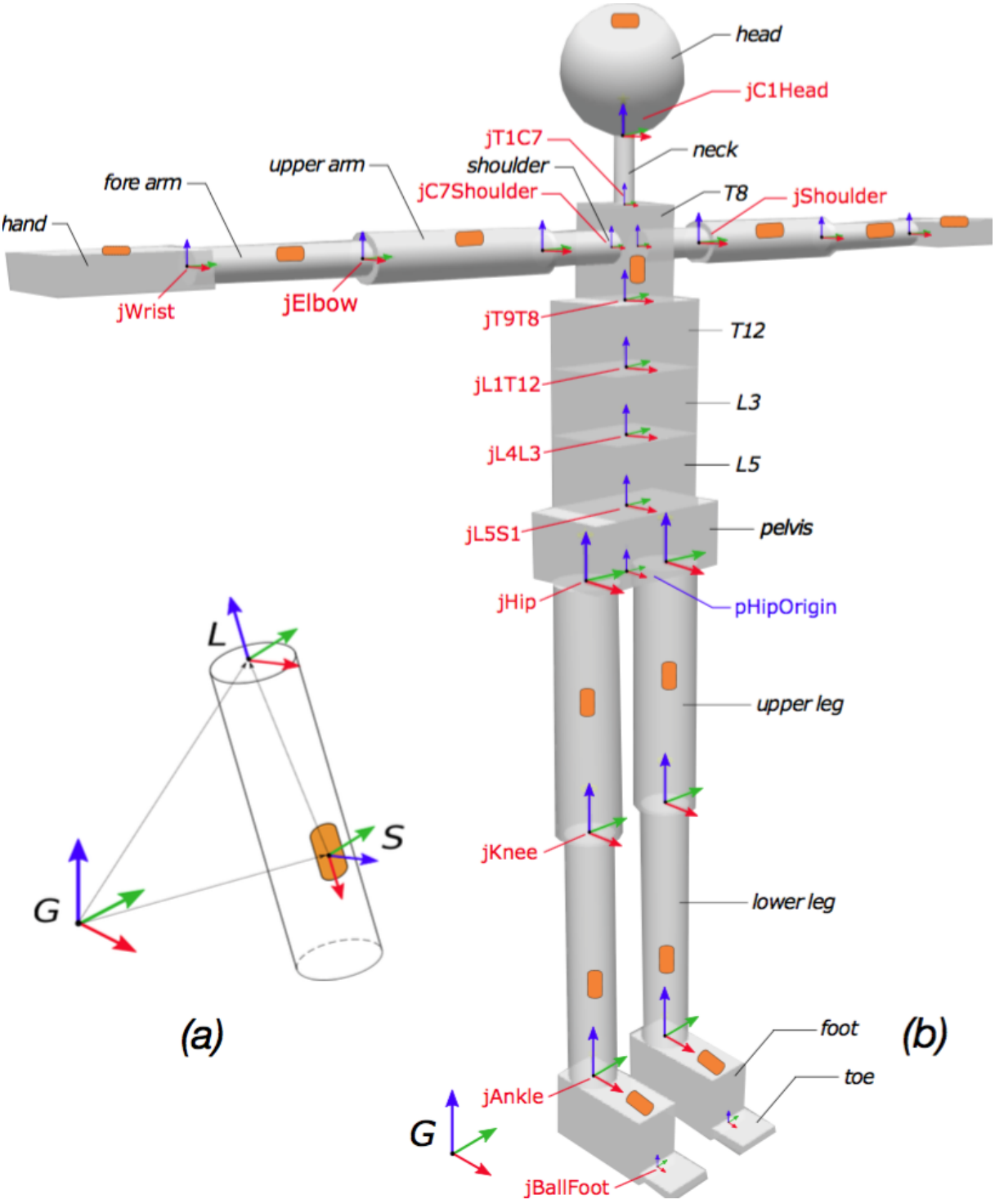

Figure 2: (a) Sensor attached to a generic link. (b) Human body reference model with labels for links and joints and with sensors distributed in the Xsens suit. Reference frames are also shown[3].

mandatory [3]. Since it is impractical to retrieve these quantities in-vivo for humans, we relied on the available anthropometric data in literature ([21], [8]) starting from the total body mass of the subject, under the assumptions of geometric approximation and of homogeneous density for the rigid bodies ([7], [23]).

4 Probabilistic Sensor Fusion Algorithm

In this Section we briefly recall the probabilistic method for estimating dynamic variables of an articulated mechanical system by exploiting the so-called sensor fusion information, already presented in our previous work (the reader should refer to [10] for a more thorough presentation).

From a theoretical point of view, we describe our model as a mechanical system represented by an oriented kinematic tree with N_B moving links and n-DoFs. Note that $n = n_1 + ... + n_{N_B}$ is the total number of DoFs of the system. The generic i-th link and its parent are coupled with a joint i following the topological Denavit-Hartenberg convention for joint numbering [2]. We are interested in computing an estimation of a vector of *dynamics variables* $\boldsymbol{d}$ defined as:

$$\begin{aligned} \boldsymbol{d} &= \begin{bmatrix} \boldsymbol{d}_1^\top & \boldsymbol{d}_2^\top & \dots & \boldsymbol{d}_{N_B}^\top \end{bmatrix}^\top \in \mathbb{R}^{24N_B+2n}, \\ \boldsymbol{d}_i &= \begin{bmatrix} \boldsymbol{a}_i^\top & \boldsymbol{f}_i^{B\top} & \boldsymbol{f}_i^\top & \boldsymbol{\tau}_i & \boldsymbol{f}_i^{x\top} & \ddot{\boldsymbol{q}}_i \end{bmatrix}^\top \in \mathbb{R}^{24+2n_i}, \end{aligned}$$

where $\boldsymbol{a}_i$ is the i-th body spatial acceleration, $\boldsymbol{f}_i^B$ is the net wrench, $\boldsymbol{f}_i$ is the internal wrench exchanged from the parent link to the i-th link, $\boldsymbol{\tau}_i \in \mathbb{R}^{n_i}$ is the torque at the joint, $\boldsymbol{f}_i^x$ is the external wrench applied by the environment to the link and $\ddot{\boldsymbol{q}}_i \in \mathbb{R}^{n_i}$ is the joint acceleration. The system can interact with the surrounding environment, and the result of this interaction is reflected in the presence of the external wrenches $\boldsymbol{f}_i^x$.

The dynamics of the mechanical system[4] can be obtained from the application of the Newton-Euler equations[5] [4]. It is possible to rearrange these equations into a matrix form thus obtaining the following linear system of equations in the variable $\boldsymbol{d}$:

$$\boldsymbol{D}(\boldsymbol{q}, \dot{\boldsymbol{q}})\boldsymbol{d} + \boldsymbol{b}_D(\boldsymbol{q}, \dot{\boldsymbol{q}}) = \boldsymbol{0}, \tag{2}$$

where the matrix $\boldsymbol{D} \in \mathbb{R}^{(18N_B+n)\times \boldsymbol{d}}$ and the bias vector $\boldsymbol{b}_D \in \mathbb{R}^{18N_B+n}$. We now consider the presence of N_S measurements of dynamic quantities coming from different sensors (e.g. accelerometers, force/torque sensors) and we denote with $\boldsymbol{y} \in \mathbb{R}^{N_S}$ the vector containing all the measurements. The dynamic variables and the values measured by the sensors can be related by the following set of equations:

$$\boldsymbol{Y}(\boldsymbol{q}, \dot{\boldsymbol{q}})\boldsymbol{d} + \boldsymbol{b}_Y(\boldsymbol{q}, \dot{\boldsymbol{q}}) = \boldsymbol{y}, \tag{3}$$

[4] We consider here the fixed base system configuration.

[5] It is worth to notice that here we prefer to adopt the Newton-Euler formalism as an equivalent representation of the system dynamics. More details about this choice in Section 3.3 of [10].

where $\boldsymbol{Y} \in \mathbb{R}^{N_S \times \boldsymbol{d}}$ and $\boldsymbol{b}_Y \in \mathbb{R}^{N_S}$. By stacking together (2) and (3) we obtain a linear system of equations in the variable $\boldsymbol{d}$:

$$\begin{bmatrix} \boldsymbol{Y}(\boldsymbol{q}, \dot{\boldsymbol{q}}) \\ \boldsymbol{D}(\boldsymbol{q}, \dot{\boldsymbol{q}}) \end{bmatrix} \boldsymbol{d} + \begin{bmatrix} \boldsymbol{b}_Y(\boldsymbol{q}, \dot{\boldsymbol{q}}) \\ \boldsymbol{b}_D(\boldsymbol{q}, \dot{\boldsymbol{q}}) \end{bmatrix} = \begin{bmatrix} \boldsymbol{y} \\ \boldsymbol{0} \end{bmatrix}. \tag{4}$$

Equation (4) describes, in general, an overdetermined linear system of equations. The bottom part, corresponding to (2) represents the Newton-Euler equations, while the upper part contains the information coming from the, possibly noisy or redundant, sensors. It is possible to compute the whole-body dynamics estimation by solving the system in (4) for $\boldsymbol{d}$. One possible approach is to solve (4) in the least-square sense, by using a Moore-Penrose pseudoinverse or a weighted pseudo-inverse.

In the following we perform a different choice. We frame the estimation of $\boldsymbol{d}$ given the knowledge of $\boldsymbol{y}$ and prior information about the model and the sensors in a Gaussian domain by means of a *Maximum-a-Posteriori* (MAP) estimator[6] such that

$$\boldsymbol{d}_{MAP} = \arg\max_{\boldsymbol{d}} p(\boldsymbol{d}|\boldsymbol{y}).$$

Since in this framework probability distributions are associated to both the measurements and the model, it suffices to compute the expected value and the covariance matrix of $\boldsymbol{d}$ given $\boldsymbol{y}$, i.e.

$$\boldsymbol{\Sigma}_{d|y} = \left(\bar{\boldsymbol{\Sigma}}_D^{-1} + \boldsymbol{Y}^\top \boldsymbol{\Sigma}_y^{-1} \boldsymbol{Y}\right)^{-1}, \tag{5a}$$

$$\boldsymbol{\mu}_{d|y} = \boldsymbol{\Sigma}_{d|y} \left[\boldsymbol{Y}^\top \boldsymbol{\Sigma}_y^{-1} (\boldsymbol{y} - \boldsymbol{b}_Y) + \bar{\boldsymbol{\Sigma}}_D^{-1} \bar{\boldsymbol{\mu}}_D\right], \tag{5b}$$

where $\bar{\boldsymbol{\mu}}_D$ and $\bar{\boldsymbol{\Sigma}}_D$ are the mean and covariance of the probability distribution $p(\boldsymbol{d}) \sim \mathcal{N}\left(\bar{\boldsymbol{\mu}}_D, \bar{\boldsymbol{\Sigma}}_D\right)$ of the model, respectively; $\boldsymbol{\Sigma}_y$ is the covariance matrix of the distribution $p(\boldsymbol{y}) \sim \mathcal{N}\left(\boldsymbol{\mu}_y, \boldsymbol{\Sigma}_y\right)$ related to the measurements. In the Gaussian framework, (5b) corresponds to the estimation of $\boldsymbol{d}_{MAP}$. It is worth noting that the vector $\boldsymbol{d}$ contains, among the other dynamic variables, an estimate of the joint torque $\boldsymbol{\tau}$ for retrieving the inverse dynamics estimation.

5 Experimental Design

In this experiment the iCub is torque controlled. The control algorithm relies on the inverse-dynamics control scheme that was presented in [17]. Human dynamics and kinematics are monitored by whole-body distributed IMU sensors and contact forces at the feet are measured with two force platforms.

5.1 Human wearable sensors for dynamic estimation

Human kinematics data were acquired by using a full-body wearable lycra suit provided by Xsens Technologies. The wearable suit is composed of 17 wired trackers,

[6] The benefits of the MAP estimator choice are explained in Section 4 of [10].

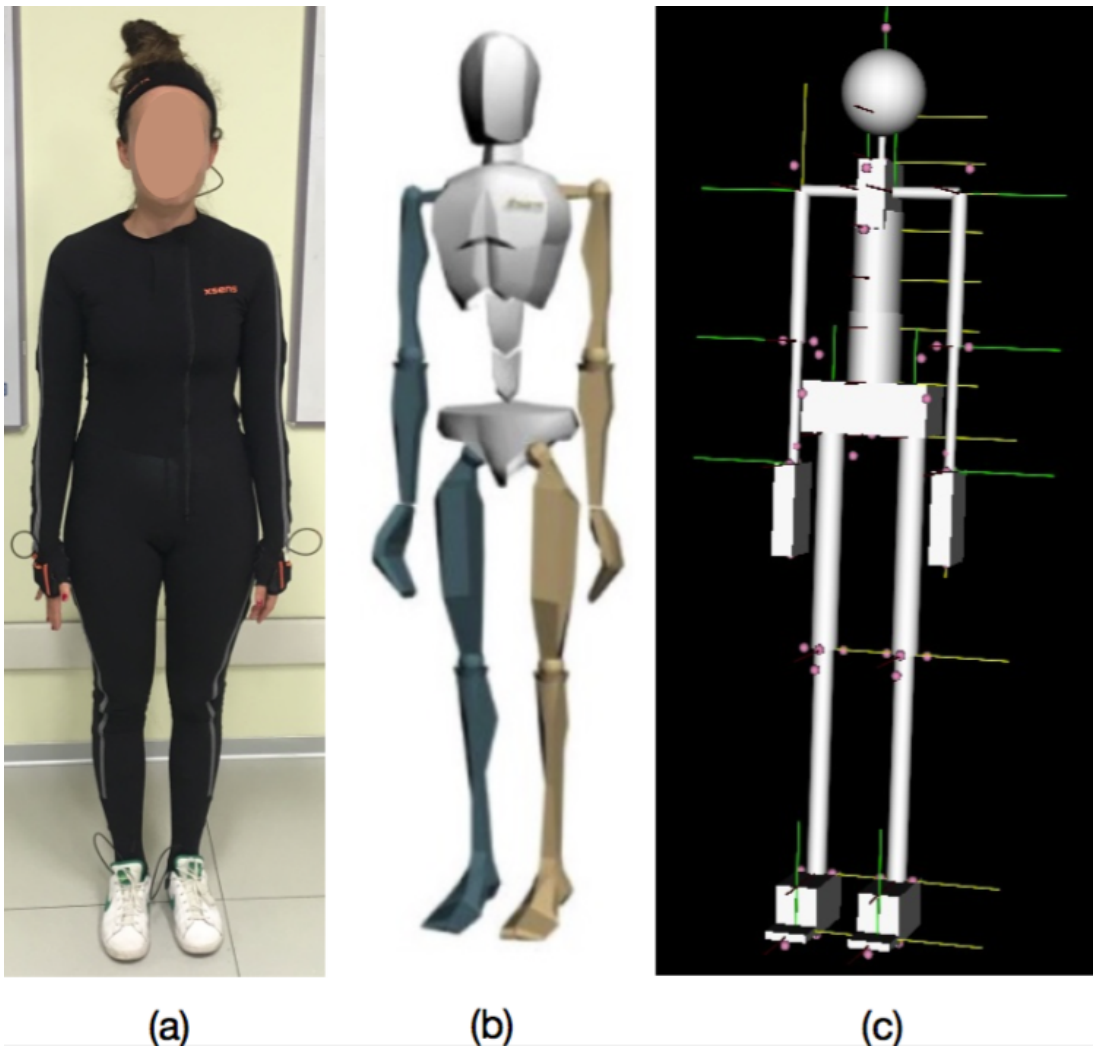

Figure 3: (a) Subject with the motion capture suit. (b) The Xsens MVN model. (c) Model reconstructed in OpenSim by using virtual markers from Xsens acquisition.

(i.e., inertial sensor units-IMUs including an accelerometer, a gyroscope and a magnetometer). The suit has signal transmitters that send measurements to the acquisition unit through a wireless receiver which collects data at a frequency of $240\ \mathrm{Hz}$. The human subject performed the required task standing with the feet on two standard force platforms AMTI OR6 mounted on the ground, while interacting with the robot. Each platform acquired a wrench sample at a frequency of $1\ \mathrm{kHz}$ by using AMTI acquisition units.

5.2 Robot sensors for dynamic estimation

Experiments were conducted on the iCub [14], a full-body humanoid robot (Fig. 4a) with 53-DoFs: 6 in the head, 16 in each arm, 3 in the torso and 6 in each leg. The iCub is endowed with whole-body distributed force/torque sensors, accelerometers, gyroscopes and tactile sensors. Specifically, the limbs are equipped with six force/torque

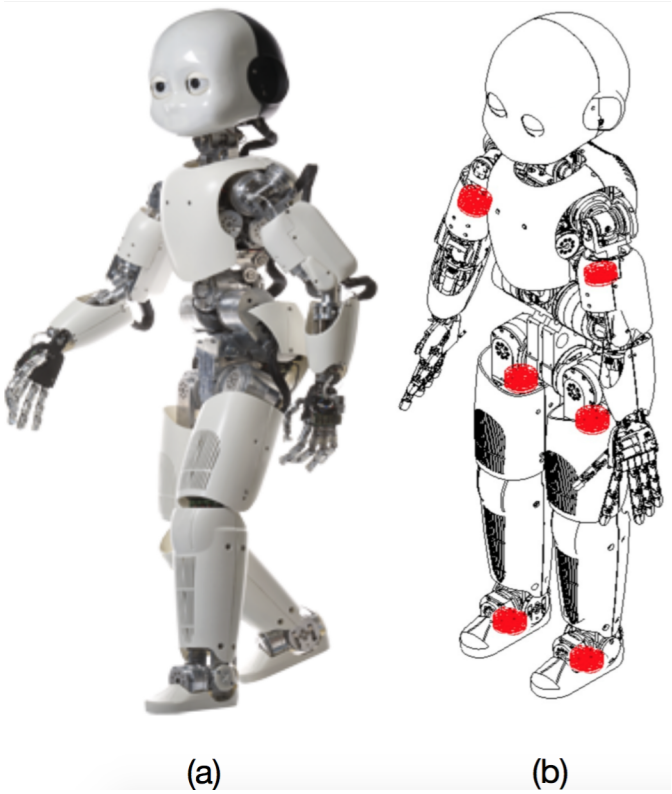

Figure 4: (a) The humanoid iCub. (b) Model of the iCub with the force/torque sensors embedded in the limbs structure.

sensors placed in the upper arms, in the upper legs and in the ankles (Fig. 4b). Internal joint torques and external wrenches are estimated through an online whole-body estimation algorithm [16]. Measurements for the wrenches exchanged between the robot and the human are obtained thanks to it. Robot data were collected at a frequency of 100 Hz.

5.3 Procedure protocol

The interacting subject (e.g. caregiver) wears the suit (Fig. 3a) and stands on the two force plates by positioning each foot on a platform. The robot is located in front of the subject, facing him and seating on a stool. It maintains balance with the whole-body inverse dynamics approach described in [17]. During the experiment, human and robot interact by exchanging forces at predefined locations. At this stage, the interaction was chosen to occur at the iCub forearm to avoid mechanical failures due to the fragility of the iCub hands (as shown in Fig. 6a). Also the relative human-robot distance is fixed by requiring the human subject to place the feet at specific locations on a printed paper which sketches the experiment layout and is placed on the floor (Fig. 6b).

The basic control strategy for the standing motion relies on whole-body inverse dynamics. The controller is implemented in Simulink[7] and has been successfully tested

[7] https://github.com/robotology-playground/WBI-Toolbox-controllers

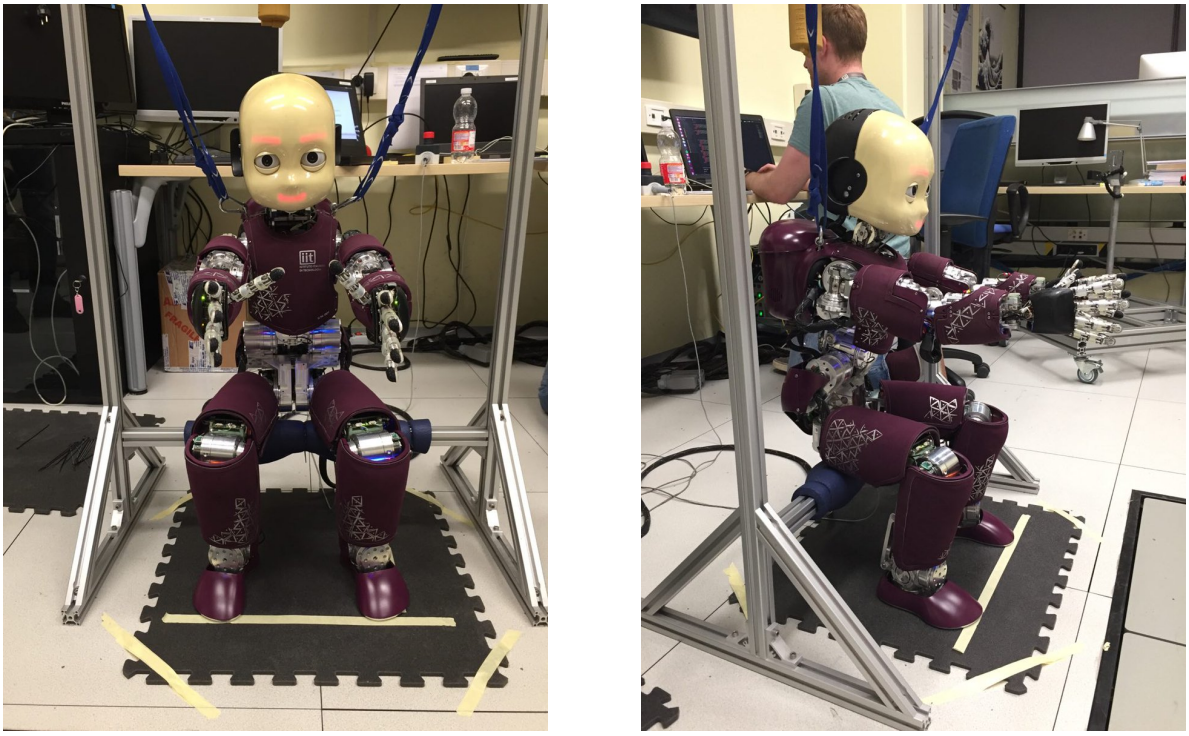

Figure 5: The iCub is initially seating on a stool while keeping the feet on the ground.

in simulation (see Fig. 7) and on the real robot (see Fig. 8). In its current version the controller performs the standing up motion without the help of the caregiver, i.e. without any physical human-robot interaction.

6 Physical human-robot interaction in Gazebo: lifting the iCub arm

To test the control software for the robot lifting with the help of the human, we first realized a prototype application in Gazebo. In this application, the robot can lift from a chair autonomously or with the help of a human; to realize a physical interaction between the human (operator, in this case) and the robot simulated in Gazebo, we used the Geomagic touch, a haptic device.

The setup consists of:

- the iCub simulation in Gazebo, complete of the dynamics information provided by *wholeBodyDynamicsTree* (`https://github.com/robotology/codyco-modules/tree/master/src/modules/wholeBodyDynamicsTree` developed by IIT in WP1) and the Cartesian information provided by *iKinCartesianController*;

- the Geomagic Touch, installed following the instructions in `https://github.com/inria-larsen/icub-manual/wiki/`

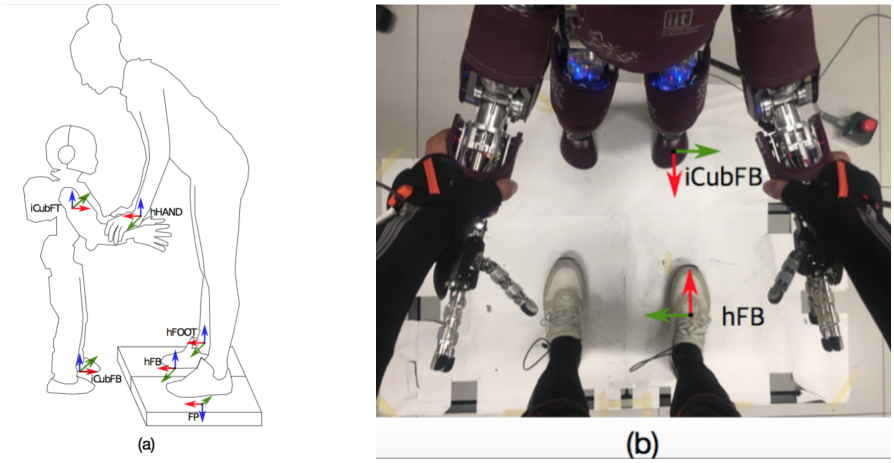

Figure 6: (a) The figure shows the reference frames for the force/torque sensor of the robot (iCubFT), the robot fixed base (iCubFB), the force plate (FP), the human fixed base (hFB), the human foot and hand (hFOOT, hHAND) respectively. (b) Top view for the feet position layout.

Figure 7: The iCub simulated standing motion without external support from a caregiver.

`Installation-with-the-Geomagic-Touch`, which not only install the SDK and drivers of the GeoMagic but also point to how to create the yarp drivers for the Geomagic;

- a C++ module (`https://github.com/inria-larsen/icubLearningTrajectories`) that connects the output command from the Geomagic to the iCub in Gazebo, and eventually enables recording the trajectories on a file.

The interconnection among the different modules is sketched in Figure 9. The tip of the Geomagic is virtually attached to the end-effector of the robot:

$$x_{geo} \rightarrow x_{icub\_hand}$$

When the operator moves the Geomagic in the space, the position of the Geomagic tip x_{geo} is scaled (1:1 by default) in the iCub workspace as x_{icub_hand}, and the Cartesian controller is used to move the iCub hand around a "home" position, or default starting position:

$$x_{icub\_hand} = hapticDriverMapping(x_0 + x_{geo})$$

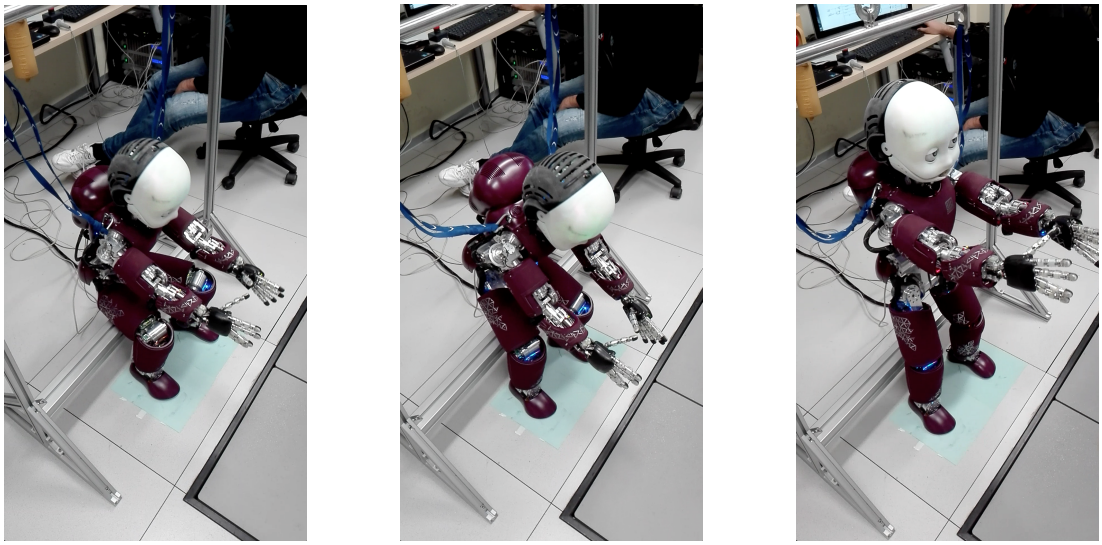

Figure 8: The iCub standing motion without external support from a caregiver.

where the *hapticDriverMapping* is the transformation applied by the haptic device driver, which basically maps the axis from the Geomagic reference frame to the iCub reference frame. By default, no force feedback is sent back to the operator in this mode, as it emulates the zero-torque control pHRI where the robot is ideally transparent and not opposing any resistance to the human guidance. A default orientation of the hand ("katana" orientation) is set.

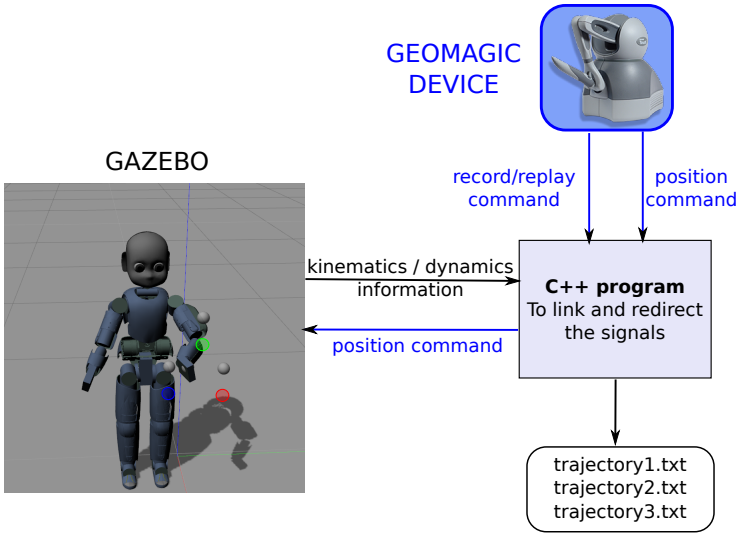

Figure 9: The interconnection between the Geomagic Touch and iCub in Gazebo.

The two buttons of the Geomagic are used to enable recording and replaying the trajectories (see Figure 10). To record a trajectory, the operator must click and hold the black button of the Geomagic; releasing the button stops recording the trajectory, and the trajectory is saved on a file (e.g., *trajectory.txt*). To replay one of the trajectories from the N previously recorded, the operator must click the light grey button of the

Geomagic and then enter the number of the trajectory on the terminal.

Figure 10: The two buttons of the Geomagic.

A video showing the iCub moved by the haptic device in Gazebo is available at this link: `https://www.youtube.com/watch?v=4ShyNtKojy0&feature=youtu.be`. The graph in Figure 11 shows some trajectories recorded from the geomagic, corresponding to lifting the left arm of the iCub: the Cartesian position of the hand in the reference frame of iCub is shown.

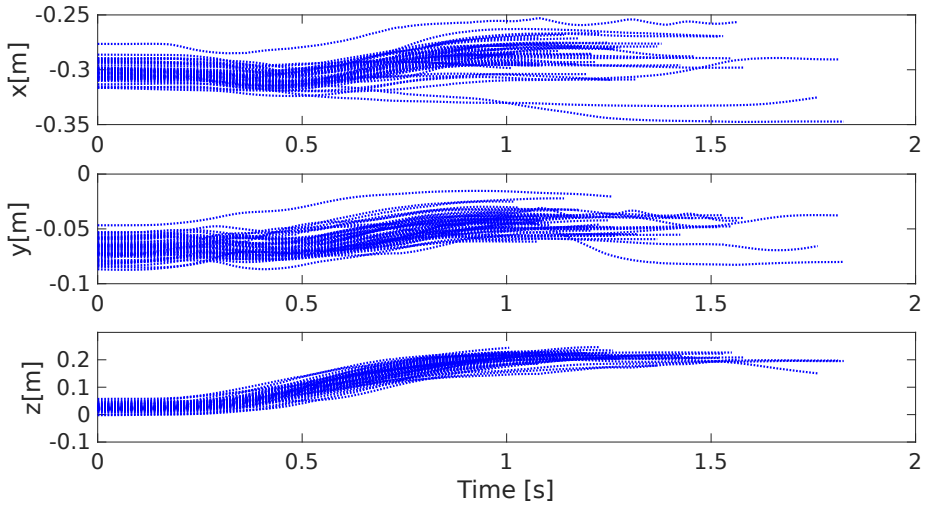

Figure 11: Some trajectories recorded when the geomagic is used to lift the left arm: Cartesian position of the end-effector.

Demonstrated trajectories and their corresponding forces can be recorded directly from the robot, by accessing the Cartesian interface and the Cartesian end-effector wrench computed by *wholeBodyDynamicsTree*.

To enable a quicker visualization of the torques and forces in action on the robot during physical interaction (in both simulation and on the real robot) we developed some visualization GUI tools `https://github.com/inria-larsen/icub-wholebody-visualization`. A major aim is to alert users, in real-time, when excessive torques are applied in one or more joints. This is especially needed when

complex interactions take place between the robot, users and the environment, such as in the case of the robot being lifted from the chair.

6.1 Learning a ProMP of the lifting movement

Once we record a set of trajectories, we can learn the distribution of these demonstration in the form of a probabilistic movement primitive (ProMP) [18]. Our toolbox for generating the proMP is currently written in Matlab, and available at `https://github.com/inria-larsen/icubLearningTrajectories`.

Let us consider the n recorded trajectories $\textcircled{\tau} = \{\tau_1, ..., \tau_n\}$, where the i-th trajectory is $\tau_i = \{y(t_1), ..., y(t_{f_i})\}$. $y(t)$ is the vector containing all the variables used to learn the ProMP, the simplest case being the mono-dimensional ProMP. If we want to learn the ProMP of the lifting motion (see Figure 11), the simplest case is $y(t) = \begin{bmatrix} z \end{bmatrix}^\top$, that is the z-axis Cartesian coordinate of the end-effector. You may notice that the duration of all the trajectories can be different, i.e., t_{f_i} may be variable across demonstrations. To be able to find a common representation in term of primitive, a temporal modulation of the trajectories is applied, such that they all have the same number of samples $\bar{s}$.

The ProMP is a Bayesian parametric model of the demonstrated trajectories in the form:

$$y(t) = \Phi(t)^\top \omega + \epsilon_y$$

where Φ are m radial basis functions scattered across time, scaled by the parameters vector $\omega \in R^m$. $\epsilon_y \sim \mathcal{N}(0, \beta)$ is the trajectory noise.

For each i-th trajectory τ_i, we compute the ω_i parameters vector:

$$y_i(t) = \Phi(t)^\top \omega_i + \epsilon_y$$

by minimizing the error between the observed trajectory $y_i(t)$ and its model $\Phi(t)^\top \omega_i + \epsilon_y$. This is done using the Least Mean Square algorithm, i.e.:

$$\omega_i = (\Phi(t)^\top \Phi(t))^{-1} \Phi(t)^\top y_i(t).$$

Then, using the aggregated $[\omega_1, ..., \omega_n]$ parameters, we can compute the distribution over these parameters $\omega \sim \mathcal{N}(\mu_\omega, \Sigma_w)$, and from this distribution, compute the distribution of the observed trajectories, which is the ProMP.

Figure 12 shows the ProMP for the lifting motion, computed with the number of reference samples $\bar{s} = 100$, number of basis functions $m = 5$; the center of each RBF is equally distributed between 1 and $\bar{s}$.

6.2 Predicting the movement from initial observations

Once the ProMP of a certain gesture has been learned (i.e., we have computed ω from $\omega_1, \ldots, \omega_n$), we can use it to predict the evolution of a movement just after few observations. Of course, the underlying hypothesis is that the movement that is observed "belongs" to the distribution of demonstrated trajectories.

Let us consider the ProMP with the parameters distribution $\omega \sim \mathcal{N}(\mu_\omega, \Sigma_\omega)$.

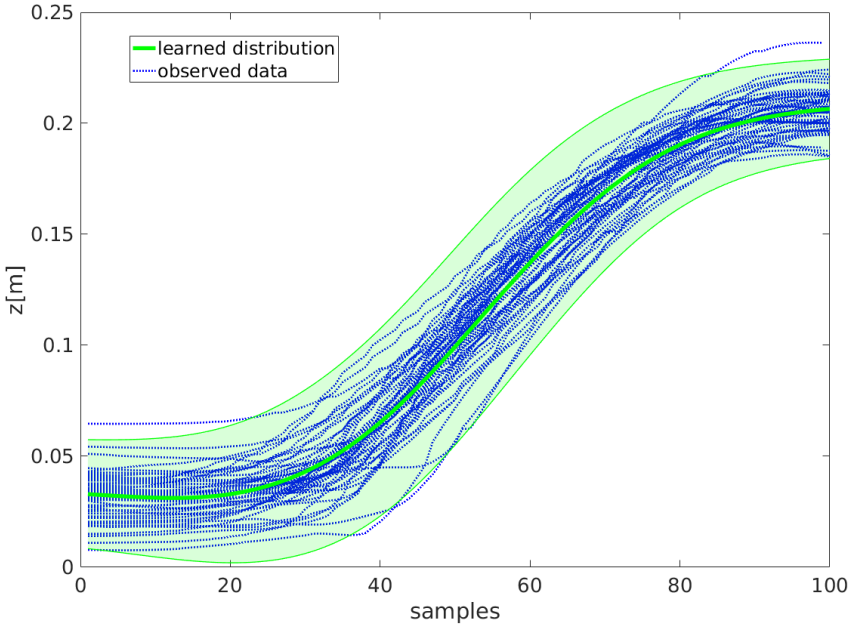

Figure 12: proMP of the left end-effector z coordinate when the arm is being lifted.

Suppose that we have n_o observations of the trajectory to predict (e.g., lifting the arm), called

$$D = [y^o(t_1), \ldots, y^o(t_{n_o})].$$

Our goal is to predict the evolution of the trajectory after t_{n_o}, i.e., find $\hat{y}(t_{n_o+1}), \ldots, \hat{y}(\hat{t}_f)$, where $\hat{t}_f$ is the estimate of the trajectory duration (by default the mean of all the $t_{f_1}, \ldots, t_{f_n}$). This is equivalent to predicting the entire trajectory $\hat{\tau}$ where the first n_o samples are known and equal to the observations: $\hat{\tau} = \{y^o(t_1), ..., y^o(t_{n_o}), \hat{y}(t_{n_o+1}), ..., \hat{y}(t_{\hat{t}_f})\}$. Therefore, our prediction problem consists in predicting $\hat{\tau}$ given the D observations. Since $\hat{\tau}$ is computed by a ProMP, finding $\hat{\tau}$ means finding the $\hat{\omega}$ generating the $\hat{\tau}$, by:

$$\begin{cases} \hat{\mu}_\omega &= \mu_\omega + K(D - \Phi_t^\top \mu_\omega) \\ \hat{\Sigma}_\omega &= \Sigma_\omega - K(\Phi_t^\top \Sigma_\omega) \\ K &= \Sigma_\omega \Phi_t^\top (\Sigma_D + \Phi_t^\top \Sigma_\omega \Phi_t)^{-1} \end{cases}$$

Figure 13 shows the predicted trajectory for the lifting motion of the left arm of iCub after $n_o = 15$. An example of the predicted trajectory for lifting the arm in Gazebo can be seen here: `https://www.youtube.com/watch?v=0i5O4Lsf7Jc&feature=youtu.be`.

7 Conclusions and Future Works

This report presents the progresses towards the implementation of learning how to stand up with the help of a human caregiver. Presented results focus on: (1) human

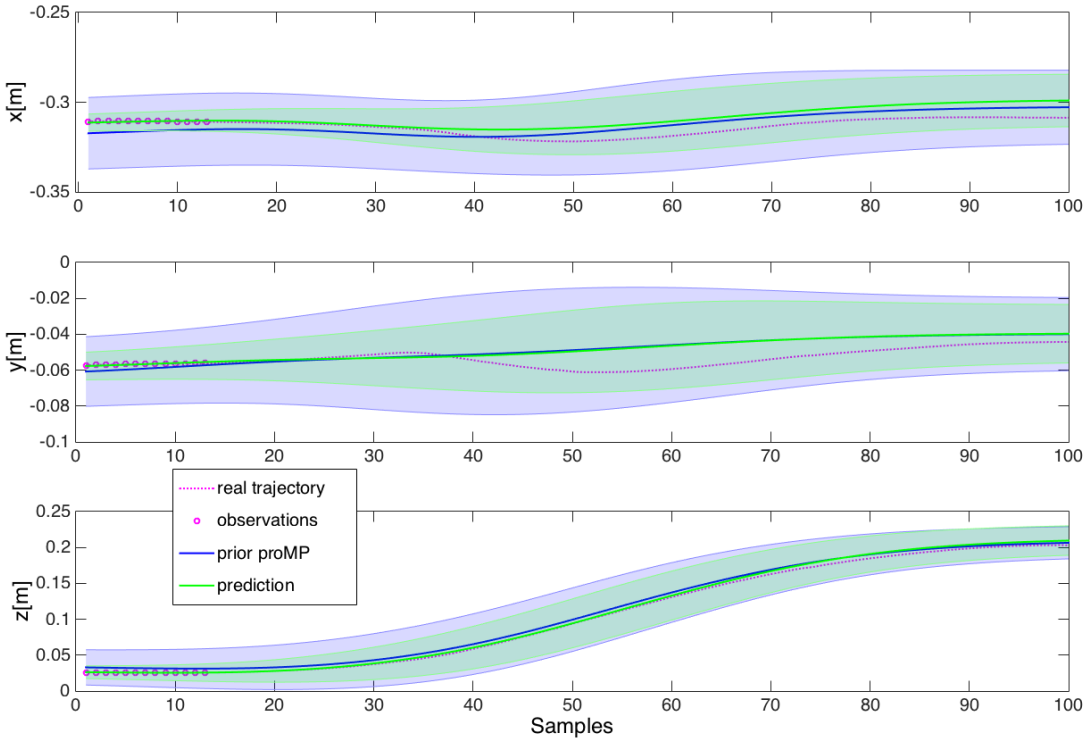

Figure 13: Prediction of the future trajectory, after $n_o = 15$ observations, given the prior proMP learned from n demonstrations.

dynamics estimation while is physically interacting with a robot; (2) robot motion control for unassisted standing up motions.

Human dynamics estimation is of pivotal importance for a control design aimed at considering the *human in the loop* during physical human robot interaction. It provides in real-time the robot with the human force feedback that could be used either as a tool for *reactive* human-robot collaboration (implying a robot reactive control) and, in a long-term perspective, for *predictive* collaboration, for enhancing remarkably the interaction naturalness. Thus, the next step consists in developing a controller to endow the robot with the ability to adapt and adjust the interaction strategy.

References

[1] H. B. Amor, G. Neumann, S. Kamthe, O. Kroemer, and J. Peters. Interaction primitives for human-robot cooperation tasks. In *2014 IEEE International Conference on Robotics and Automation (ICRA)*, pages 2831–2837, May 2014.

[2] J. Denavit and R. S. Hartenberg. A kinematic notation for lower-pair mechanisms based on matrices. *Trans. of the ASME. Journal of Applied Mechanics*, 22:215–221, 1955.

[3] R. Drillis, R. Contini, and M. Bluestein. Body segment parameters; a survey of measurement techniques. *Artificial limbs*, 25, 1964.

[4] R. Featherstone. *Rigid Body Dynamics Algorithms*. Springer-Verlag New York, Inc., Secaucus, NJ, USA, 2007.

[5] T. Flash and N. Hogan. The coordination of arm movements: an experimentally confirmed mathematical model. *Journal of Neuroscience*, 5(7):1688–1703, 1985.

[6] G. Guerra-Filho and A. Biswas. The human motion database: A cognitive and parametric sampling of human motion. In *Face and Gesture 2011*, pages 103–110, March 2011.

[7] E. P. Hanavan. A mathematical model of human body. Technical report, Air force aerospace medical research lab Wright-Patterson AFB OH, 1964.

[8] I. P. Herman. *Physics of the human body*, chapter Terminology, the standard human, and scaling. Springer, 2007.

[9] H. Kuehne, H. Jhuang, E. Garrote, T. Poggio, and T. Serre. Hmdb: A large video database for human motion recognition. In *2011 International Conference on Computer Vision*, pages 2556–2563, Nov 2011.

[10] C. Latella, N. Kuppuswamy, F. Romano, S. Traversaro, and F. Nori. Whole-body human inverse dynamics with distributed micro-accelerometers, gyros and force sensing. *Sensors*, 16(5):727, 2016.

[11] Y. Maeda, T. Hara, and T. Arai. Human-robot cooperative manipulation with motion estimation. In *Intelligent Robots and Systems, 2001. Proceedings. 2001 IEEE/RSJ International Conference on*, volume 4, pages 2240–2245, 2001.

[12] C. Mandery, Ö. Terlemez, M. Do, N. Vahrenkamp, and T. Asfour. Unifying representations and large-scale whole-body motion databases for studying human motion. *IEEE Transactions on Robotics*, 32(4):796–809, Aug 2016.

[13] J. E. Marsden and T. S. Ratiu. *Introduction to Mechanics and Symmetry: A Basic Exposition of Classical Mechanical Systems*. Springer Publishing Company, Incorporated, 2010.

[14] G. Metta, L. Natale, F. Nori, G. Sandini, D. Vernon, L. Fadiga, C. von Hofsten, K. Rosander, M. Lopes, J. Santos-Victor, A. Bernardino, and L. Montesano. The icub humanoid robot: An open-systems platform for research in cognitive development. *Neural Networks*, 23(8–9):1125 – 1134, 2010. Social Cognition: From Babies to Robots.

[15] S. Miossec and A. Kheddar. Human motion in cooperative tasks: Moving object case study. In *Robotics and Biomimetics, 2008. ROBIO 2008. IEEE International Conference on*, pages 1509–1514, Feb 2009.

[16] F. Nori, S. Traversaro, J. Eljaik, F. Romano, A. Del Prete, and D. Pucci. icub whole-body control through force regulation on rigid non-coplanar contacts. *Frontiers in Robotics and AI*, 2015.

[17] F. Nori, S. Traversaro, J. Eljaik, F. Romano, A. Del Prete, and D. Pucci. icub whole-body control through force regulation on rigid noncoplanar contacts. *Frontiers in Robotics and AI*, 2(6), 2015.

[18] A. Paraschos, C. Daniel, J. Peters, and G. Neumann. Probabilistic movement primitives. In *Advances in Neural Information Processing Systems (NIPS)*. mit press, 2013.

[19] D. Roetenberg, H. Luinge, and P. Slycke. Xsens mvn: full 6dof human motion tracking using miniature inertial sensors. Technical report, Xsens Motion Technologies BV, 2009.

[20] Ö. Terlemez, S. Ulbrich, C. Mandery, M. Do, N. Vahrenkamp, and T. Asfour. Master motor map (mmm) - framework and toolkit for capturing, representing, and reproducing human motion on humanoid robots. In *2014 IEEE-RAS International Conference on Humanoid Robots*, pages 894–901, Nov 2014.

[21] D. A. Winter. *Biomechanics and motor control of human movement*, chapter Anthropometry. Wiley, 1990.

[22] J. Wojtusch and O. von Stryk. Humod - a versatile and open database for the investigation, modeling and simulation of human motion dynamics on actuation level. In *2015 IEEE-RAS 15th International Conference on Humanoid Robots (Humanoids)*, pages 74–79, Nov 2015.

[23] M. Yeadon. The simulation of aerial movement ii. a mathematical inertia model of the human body. *Journal of Biomechanics*, 23(1):67–74, 1990.